

1 **Photoinactivation of Bacteria Attached to Glass and Acrylic Surfaces by 405 nm Light:**
2 **Potential Application for Biofilm Decontamination**

3

4 Karen McKenzie*, Michelle Maclean, Igor V. Timoshkin, Endarko Endarko,
5 Scott J. MacGregor, John G. Anderson

6

7

8 *Corresponding author. Mailing address: ROLEST, Department of Electronic and Electrical
9 Engineering, University of Strathclyde, Royal College Building, 204 George Street, Glasgow,
10 Scotland, G1 1XW. Phone:+44(0)141 548 2376. Fax:+44(0)141 552 5398.

11 E-mail: karen.mckenzie@strath.ac.uk

12

13

14

15

16

17

18

19

20

21

22

23

24

25

26 **ABSTRACT**

27

28 Attachment of bacteria to surfaces and subsequent biofilm formation remains a major cause
29 of cross contamination capable of inducing both food related illness and nosocomial
30 infections. Resistance to many current disinfection technologies means facilitating their
31 removal is often difficult. The aim of this study was to investigate the efficacy of 405 nm
32 light for inactivation of bacterial attached as biofilms to glass and acrylic. *Escherichia coli*
33 biofilms (10^3 - 10^8 cfu mL⁻¹) were generated on glass and acrylic surfaces and exposed for
34 increasing times to 405 nm light (5-60 minutes) at ~140mW cm⁻². Successful inactivation of
35 biofilms has been demonstrated, with results highlighting complete/near complete
36 inactivation (up to 5 log₁₀ reduction on acrylic and 7 log₁₀ on glass). Results also highlight
37 inactivation of bacterial biofilms could be achieved whether the biofilm was on the upper
38 'directly exposed' surface or 'indirectly exposed' underside surface. Statistically significant
39 inactivation was also shown with a range of other microorganisms associated with biofilm
40 formation (*Staphylococcus aureus*, *Pseudomonas aeruginosa* and *Listeria monocytogenes*).
41 Results from this study have demonstrated significant inactivation of bacteria ranging from
42 monolayers to densely populated biofilms using 405 nm light, highlighting that with further
43 development, this technology may have potential applications for biofilm decontamination in
44 food and clinical settings.

45

46

47 Key words: biofilms; disinfection; antimicrobial; visible light; bacteria

48

49

50

51 **INTRODUCTION**

52

53 Bacterial attachment to surfaces under the correct environmental conditions often leads to
54 biofilm formation. The structure of a biofilm can range from simple monolayers to vast
55 complex multicellular structures, either of single or mixed species and can act as a protective
56 barrier against hostile environmental conditions providing resistance to both physical and
57 chemical stresses (1,2,3,4)

58

59 Biofilm formation is a well-recognised problem within food and healthcare industries, with
60 their presence having detrimental effects on both food quality and safety, and infection
61 control. Multiple bacterial species including *Escherichia coli*, *Salmonella*, *Staphylococcus*,
62 *Listeria* and *Pseudomonas* are all capable of attaching and inducing biofilm formation on
63 various surfaces including metals, glass and plastics (5,6), allowing for a continuous bacterial
64 reservoir often leading to further contamination.

65

66 Food production premises provide an ideal environment for biofilm formation. These, often
67 moist, environments have a continuous supply of nutrients from various food products, as
68 well as vast surface areas for attachment and continuous supply of inoculum to initiate
69 biofilm formation (1,7,8). Their existence in food environments is not only problematic in
70 terms of consumer health but also has massive financial implications in terms of product loss,
71 justifying the need for investment in novel disinfection technologies.

72

73 Within clinical environments formation of microbial biofilms is a notable problem,
74 contributing to the transmission of hospital acquired infections. It has been suggested that the
75 presence of patient fluids such as blood, urine and saliva influence bacterial adhesion and

76 biofilm development (5). A recent study highlighted the presence of *P. aeruginosa* biofilms
77 on sink areas directly resulted in 36 patients acquiring infection of which a 33% death rate
78 was observed (9). Further studies have demonstrated that biofilm formation on indwelling
79 medical devices and implanted prosthetics may account for up to 25% of patient morbidity
80 and mortality, with over one million related infections in the United States in 2010 (10,11).

81

82 Numerous decontamination technologies have been developed and integrated into industry to
83 help minimise microbial contamination. Methods for reducing microbial contamination such
84 as chemical disinfection are still heavily used, however poor penetrability of chemical agents
85 through biofilms is a major limitation, allowing bacterial survival, re-dispersal and further
86 contamination (2,12,13). The continuous use of biocides, often at sub-lethal concentrations is
87 an important factor contributing to bacterial resistance, limiting the availability of effective
88 disinfectant agents (14). Genetic adaptations in many bacterial species has led to the
89 development of resistance against many chemical cleaning agents, thereby preventing
90 sufficient disinfection and increasing the potential risk of pathogen transmission (14,15).
91 Consequently many biocides are failing to effectively disinfect open work surfaces and novel
92 methods of decontamination are continually being sought.

93

94 Recent studies have demonstrated the bactericidal properties of violet-blue 405 nm light
95 against a range of both Gram-positive and Gram-negative bacterial species
96 (16,17,18,19,20,21,22,23,24). Although not as bactericidal as ultraviolet light, 405 nm light
97 has benefits relating to its higher safety and increased transmissibility. Photodynamic
98 inactivation (PDI) of bacteria by exposure to 405 nm light has been attributed to the
99 excitation of intracellular photosensitive porphyrin molecules. Excitation of these molecules

100 with 405 nm light, results in the production of reactive oxygen species (ROS), most
101 predominately singlet oxygen, and consequently oxidative damage and cell death (18,22).

102

103 Previous studies utilising 405 nm light for inactivation of bacterial pathogens have
104 demonstrated significant reductions of bacterial populations both in liquid suspension and
105 seeded onto solid surfaces (20,23,25). This study investigates for the first time the significant
106 bactericidal effect of 405 nm light on *E. coli* biofilms of varying maturity, generated on glass
107 and acrylic surfaces. The transmissibility of 405 nm light is demonstrated by successful
108 inactivation of bacterial biofilms after transmission through the transparent glass and acrylic
109 surfaces. Results also highlight the effect of 405 nm light for inactivation of biofilms of other
110 problematic biofilm-forming bacteria including *Pseudomonas aeruginosa*, *Staphylococcus*
111 *aureus* and *Listeria monocytogenes*.

112

113

114 MATERIALS AND METHODS

115

116 **Bacterial Preparation:** The bacteria used in this study were: *Escherichia coli* NCTC 9001;
117 *Staphylococcus aureus* NCTC 4135 (obtained from National Collection of Type Cultures,
118 Colindale UK); *Listeria monocytogenes* LMG 19944; and *Pseudomonas aeruginosa* LMG
119 9009 (obtained from the Laboratorium voor Microbiologie, Universiteit Gent, Belgium).
120 Bacteria were incubated in 100 mL nutrient broth (*E. coli*, *S. aureus* and *P. aeruginosa*) or
121 tryptone soya broth (*L. monocytogenes*), (Oxoid Ltd, UK) at 37°C for 18 hours under rotary
122 conditions (120 rpm). Broths were then centrifuged at 3939×g for 10 minutes, and the cell
123 pellets re-suspended in 100 mL phosphate buffer saline (PBS; Oxoid Ltd, UK), and diluted to
124 a population density of 10⁷ CFU mL⁻¹ for experimental use.

125 **Biofilm Formation:** Biofilms were prepared on glass and acrylic slides (60 × 25 mm). These
126 materials were selected for two reasons: (i) they represent hydrophilic and hydrophobic
127 surfaces, respectively, and (ii) their transparency allowed transmission of the 405 nm light.
128 To prepare biofilm samples, glass and acrylic slides were first cleaned with ethanol to
129 sterilise and remove grease. For development of single species monolayer biofilms, for both
130 direct and indirect exposure, slides were fully immersed in 125 mL 10⁷ CFU mL⁻¹ bacterial
131 suspension for 1 hour to facilitate initial attachment. The bacterial suspension was then
132 discarded and replaced with growth media (1.0 g bacteriological peptone and 0.7 g yeast
133 extract l⁻¹ in sterile distilled water) in which the slides were left for a further 4 hours to allow
134 development of a monolayer biofilm (method adapted from (1)). For development of more
135 mature biofilms, slides were left in the growth media for increasing time periods (24, 48, 72
136 hours). After biofilm development, slides were aseptically removed from the growth media
137 and left to dry for 10 minutes in sterile conditions at room temperature prior to light
138 exposure. For development of mixed species biofilms, slides were immersed in a 125 mL 10⁷
139 CFU mL⁻¹ bacterial suspension containing 62.5 mL *E. coli* suspension and 62.5 mL *S. aureus*
140 suspension for 1 hour. Slides were then placed in growth media for a further 24 hours to
141 allow sufficient biofilm formation.

142

143 **405 nm Light Source:** An ENFIS Quattro Mini Air Cooled Light Engine (ENFIS Ltd, UK),
144 containing an array of 144 light emitting diodes (LED) with a light emission of 405 nm
145 (±5 nm) was used for exposure of bacterial biofilms. The light engine incorporated a heat
146 sink and cooling fan to permit continuous ventilation and prevent overheating of the LED
147 array, and was powered by a 48V power supply. For exposure, biofilm sample slides were
148 positioned directly below the LED array at a distance of 5 cm. Irradiance from the LED array
149 at this distance was measured using a radiant power meter and photodiode detector (LOT

150 Oriel, USA). The variation of irradiance was measured across the dimensions of the slide,
151 and measurements indicated greatest irradiance at the midpoint of the slide, with a gradual
152 decrease towards the outer edges (Figure 1). The average irradiance across the entire slide
153 surface was calculated, using OriginPro 8.1 software package, to be $141.48 \text{ mW cm}^{-2}$. Test
154 samples were light exposed for 5-60 minutes, giving a range of average doses from 42 J cm^{-2}
155 to 504 J cm^{-2} . Control slides were set up and left on the laboratory bench with no 405 nm
156 illumination.

157

158 <FIGURE 1>

159

160 In addition to directly exposing biofilms, the potential for 405 nm light to transmit through
161 glass and acrylic slides and inactivate biofilms on the underside of slides was investigated. To
162 do this, it was important to determine the transmissibility of the light through these slides.
163 This was measured by placing the power meter detector head on the underside of the exposed
164 surfaces: transmission of the 405 nm light through these materials was found to result in an
165 approximate 4% loss in irradiance.

166

167

168 **Swabbing and Enumeration:** Following light exposure, surviving bacteria were recovered
169 from the slide using a sterile cotton-tipped swab moistened in PBS. The swabbing procedure
170 involved rolling the swab forward and backward multiple times across the entire surface of
171 the illuminated side of the slide to ensure maximum recovery of bacterial biofilm sample (1).
172 This protocol was kept consistent for all sample slides. The swab was then immersed in a
173 10 mL volume containing 9 mL PBS and 1 mL 3% Tween-80 suspension and vortexed for 1
174 minute to allow re-suspension of bacteria from swab into suspension. The suspension was

175 serially diluted, by transfer of 1 mL volumes into 9 mL of PBS. Samples were plated using
176 the pour plate method, with 1 mL sample volumes overlaid with nutrient agar (*E. coli*,
177 *S. aureus* and *P. aeruginosa*) or tryptone soya agar (*L. monocytogenes*): this method provided
178 a detection limit of 1 CFU mL⁻¹. For enumeration of bacteria in a mixed biofilm population,
179 in addition to pour-plating samples in nutrient agar to obtain the total viable counts (TVC),
180 bacterial samples (100µl-500µl) were plated onto mannitol salt agar (MSA) and violet red
181 bile agar (VRBA), which allowed the selective growth of *S. aureus* and *E. coli*, respectively.
182 Plates were then incubated at 37°C for 18-24 hours. Plates were enumerated manually by
183 counting the bacterial colony-forming units (CFU) present on the plate. Results in Figures are
184 reported as bacterial CFU count per millilitre (log₁₀ CFU mL⁻¹) as a function of time
185 (minutes).

186

187 **Statistical Analysis:** Experimental data is an average of a minimum of triplicate independent
188 experimental results, with triplicate samples taken from each experiment. All data were
189 analysed using one way ANOVA test with Minitab 15 statistical software, where significant
190 difference was accepted at P < 0.05. Weibull statistics (26) were used to analyse the
191 inactivation behaviour of monolayer bacterial biofilms cultured on glass and acrylic surfaces,
192 methodology for this analysis is described later.

193

194

195

196

197

198

199

200 RESULTS

201

202 Inactivation of *E. coli* biofilms on glass and acrylic surfaces

203

204 Results have demonstrated that *E. coli* biofilms on glass and acrylic surface materials can be
205 successfully inactivated by 405 nm light exposure. Figure 2 show results for the inactivation
206 of *E. coli* biofilms on glass. The most rapid inactivation was observed with *E. coli* monolayer
207 biofilms, with a 2.52 log₁₀ CFU mL⁻¹ reduction following 10 minutes exposure, and complete
208 kill (3.55 log₁₀ CFU mL⁻¹ reduction) following 20 minutes exposure, as shown by the 4-hour
209 trendline on Figure 2. After 24 hours in the growth medium, bacterial biofilm populations on
210 glass were shown to be approximately 5.7 log₁₀ CFU mL⁻¹. Inactivation of these biofilms
211 occurred at a relatively linear rate, with reductions of 2.27, 4.41 and 5.7 log₁₀ CFU mL⁻¹
212 following exposure to 20, 30 and 40 minutes respectively. Biofilms on glass developed over
213 48 and 72 hour periods had increased cell densities, with starting populations of between 7-8
214 log₁₀ CFU mL⁻¹ prior to light exposure. The rate of inactivation for these biofilms was very
215 similar, with 3-3.5 log₁₀ CFU mL⁻¹ reductions achieved when exposed for 20 minutes, and a
216 further ~2 log₁₀ CFU mL⁻¹ reduction after a further 20 minutes. Near complete inactivation of
217 the 48-hour biofilms and complete inactivation (<1 CFU mL⁻¹ surviving) of the 72-hour
218 biofilms was achieved following 60 minutes exposure to 405 nm light.

219

220 <FIGURE 2>

221

222 Figure 3 demonstrates the inactivation kinetics of *E. coli* biofilms on acrylic.
223 Monolayer biofilms on acrylic surfaces were reduced by approximately 0.5 log₁₀ CFU mL⁻¹
224 after 10 minutes exposure, significantly less (P=0.002) than the 2.52 log₁₀ CFU mL⁻¹

225 reduction observed on glass. After 15 minutes exposure, there was however a $3.33 \log_{10}$
226 CFU mL^{-1} reduction in the biofilm population on acrylic, statistically similar to that achieved
227 on glass at the same time point. After 24 hours of biofilm development, bacterial populations
228 were approximately $4.7 \log_{10} \text{CFU mL}^{-1}$ on acrylic slides. Biofilm inactivation occurred at a
229 steady and consistent rate when applied with increasing exposure times of 405 nm light (20,
230 30, 40 and 60 minutes), resulting in reductions of 2.30, 3.07, 3.67 and $4.69 \log_{10} \text{CFU mL}^{-1}$,
231 respectively. Development of biofilms over a 48 hour period generated a bacterial population
232 of $\sim 5.1 \log_{10} \text{CFU mL}^{-1}$, where near complete inactivation was achieved following exposure
233 for 60 minutes ($< 1 \text{CFU mL}^{-1}$). Bacterial biofilm formation on acrylic surfaces after 72 hours
234 growth period demonstrated no significant increase in bacterial count from that recorded after
235 48 hour growth period ($P = 0.06$), therefore biofilms grown for 72 hours on acrylic were not
236 investigated.

237

238 <FIGURE 3>

239

240 The population densities of all non-exposed control biofilm samples, on both glass
241 and acrylic, remained consistent throughout, with no significant differences recorded over the
242 duration of the experiment, indicating that inactivation was a direct result of 405 nm light
243 exposure. It is likely that the reason for no loss of viability in the control populations was due
244 to the relatively short periods involved (up to 1 hour periods) as well as the protective effect
245 of the biofilm structure.

246

247 It is also worth noting that no significant temperature build up was observed on test
248 samples during light exposure. Temperatures of both glass and acrylic surfaces were
249 measured across the slide to give accurate representation of heat distribution across the entire

250 area. For each material, temperatures were measured after maximum exposure periods using
251 a thermocouple, which was pressed onto the test surface. The maximum temperature recorded
252 was 33°C, indicating bacterial kill was not a result of direct thermal kill or desiccation
253 through prolonged heat treatment.

254

255

256 **Inactivation of *E. coli* monolayer biofilms through transmissible materials**

257 Experiments were carried out to establish whether the 405 nm light could transmit through
258 the glass and acrylic and inactivate biofilms on the underside of the slides. For ‘indirect’
259 biofilm exposure, after removal from the growth medium, the upper side of the slide was
260 wiped clean to ensure biofilm formation was only on the underside of the slide. The
261 inactivation data for these ‘indirectly’ exposed biofilms is presented in Figures 4a and 4b as a
262 comparison to the directly exposed biofilms.

263

264 Glass microscope slides have high transmittance in the visible light region around 400
265 nm. As a result, there was negligible differences between the inactivation for both direct and
266 indirectly exposed biofilms on glass slides as can be seen from Figure 4a,. There was no
267 significant difference ($P= 0.738$) between the direct and indirect \log_{10} CFU mL⁻¹ reductions
268 following 10 minutes exposure, and complete inactivation (<1 CFU mL⁻¹ survivors) was
269 achieved for both samples after 20 minutes exposure. Similarly, Figure 4b demonstrated
270 similar inactivation curves for both direct and indirect exposure of biofilms on acrylic, with
271 no significant difference in the population reductions achieved with direct and indirect
272 exposure after 10 minutes ($P=0.421$) and 20 minutes ($P=0.507$) which also indicates that the
273 acrylic slides used in the present work transmit well visible 405 nm light. As noted,
274 irradiance measurements determined that transmission of the 405 nm light through the glass

275 and acrylic slides with monolayer growth, resulted in an approximate 4% reduction in
276 irradiance, however, this reduction was insufficient to cause significant differences in the
277 inactivation rates of the directly and indirectly exposed biofilms on either the glass or the
278 acrylic surfaces.

279 <FIGURE 4>

280

281 **Weibull Analysis**

282

283 The inactivation behaviour of monolayer bacterial biofilms grown on glass and acrylic
284 surfaces was analysed using the Weibull statistical approach, which can help in the
285 identification of potential differences in inactivation mechanisms. The Weibull distribution
286 has been employed for the analysis of microbial inactivation kinetics, including PDI studies
287 (27,28), however, a paper by Schenk et al. (29) which investigates UV microbial inactivation,
288 states that “there is no information about the application of a Weibullian-type model to
289 survival curves corresponding to microorganisms inoculated onto a solid surface”. Therefore,
290 it was interesting to examine the potential applicability of this statistical model to 405 nm
291 light inactivation of biofilms cultured on solid surfaces.

292

293 In the Weibull’s approach, the 405 nm light dose, D_c , which is required to kill a single
294 microorganism from an entire population is considered as a measure of resistance of this
295 organism to the light. It is also assumed that D_c is Weibull distributed. The survival rate of
296 microorganisms which form biofilms, $S(D)$, is defined as the number of microorganisms
297 surviving at a specific 405 nm light dose, $N(D)$, divided by the initial number of
298 microorganisms, N_0 :

$$299 \quad S(D) = N(D)/N_0 \quad (1)$$

300 In these conditions the survival rate, $S(D)$, can be described by the Weibull's cumulative
301 distribution function, (26) and satisfies the following equation:

$$302 \log_{10}(S(D)) = -0.4343 \alpha D^\beta \quad (2)$$

303 where α and β are parameters of the Weibull distribution.

304

305 Experimental inactivation data for monolayer biofilms on acrylic and glass surfaces
306 exposed to direct and indirect 405 nm light have been represented as $\log_{10}(S(D))$. These
307 experimental data points and corresponding analytical fit lines obtained by Equation (2) are
308 shown in Figures 4a and 4b (inset graphs). Analytical lines show downward concavity for
309 the acrylic surface and upward concavity for the glass surface.

310

311 Coefficient β which determines the shape of the Weibull's distribution has been
312 obtained for both surfaces and both types of the light treatment as shown in Figure 4. For
313 acrylic surfaces (Figure 4a) the shape parameter, β , is higher than 1: $\beta = 3$ in the case of the
314 direct exposure and $\beta = 3.6$ in the case of the indirect exposure. $\beta > 1$ indicates that with an
315 increase in 405 nm light dose, microorganisms in the biofilm become increasingly damaged
316 and can be killed at a higher rate. In the case of the glass surface (Figure 4b) the shape
317 parameter is smaller than 1: $\beta = 0.378$ and $\beta = 0.396$ for direct and indirect exposures
318 respectively. $\beta < 1$ means that the rate of inactivation is higher at lower 405 nm light doses,
319 and this rate decreases with an increase in the light dose. Potentially such inactivation
320 behaviour may indicate that remaining (surviving) microorganisms in the biofilm become
321 more resistive to the external stress (405 nm light).

322

323

324

325 **Comparison of the inactivation of different bacterial monolayer biofilms on glass**
326 **surfaces**

327

328 As a comparison to *E. coli*, the bactericidal efficacy of 405 nm light was tested against a
329 range of other bacterial biofilms. *S. aureus*, *L. monocytogenes* and *P. aeruginosa* monolayer
330 biofilms attached to glass surfaces were exposed to 5, 10 and 20 minutes of 405 nm light to
331 determine the comparative levels of bacterial inactivation. Using the stipulated 4-hour
332 development period, it was found that the initial starting populations varied considerably
333 between the different bacterial species, with higher populations found for the Gram-positive
334 species. Results in Table 1 show that successful bactericidal effects were recorded with all
335 the tested biofilms. Initial exposure for 5 minute, resulted in between 0.6-1.5 log₁₀ CFU mL⁻¹
336 reductions for *S. aureus*, *L. monocytogenes* and *P. aeruginosa*, whereas at the same time
337 point little change in population was observed for the *E. coli* biofilms. After 10 minutes
338 exposure, 405-nm light achieved a 2.4-2.5 log₁₀ CFU mL⁻¹ reduction in bacterial population
339 in both *E. coli* and *P. aeruginosa*, compared to 1.1 and 1.9 log₁₀ CFU mL⁻¹ reductions in *L.*
340 *monocytogenes* and *S. aureus* biofilms, respectively. Overall, the population reductions
341 achieved following 20 minutes exposure were similar between the two Gram-negative
342 bacteria (~3.6 log₁₀ CFU mL⁻¹), with which complete inactivation was achieved, and between
343 the two Gram-positive bacteria (~2.6 log₁₀CFU mL⁻¹).

344

345

346 <TABLE 1>

347

348

349

350 **Inactivation of mixed species biofilms**

351

352 Mixed species biofilms containing both *E. coli* and *S. aureus* were prepared on glass slides.
353 Confirmation of the mixed population was obtained by microscopic view (Figure 5) of a
354 biofilm slide which had been Gram-stained in order to visualise the presence of both *E. coli*
355 (pink rods) and *S. aureus* (purple cocci). Table 2 displays results from the exposure of these
356 mixed biofilm populations, and also single-species complex biofilms (24h growth period) of
357 *E. coli* and *S. aureus*, to 405 nm light. Results show that after a 30-minute exposure period,
358 significant inactivation was achieved in all cases. Exposure of single species biofilms
359 induced a 4.37 log₁₀ CFU mL⁻¹ reduction in *E. coli* and a 2.97 log₁₀ CFU mL⁻¹ reduction in
360 *S. aureus* biofilms. Successful inactivation was also observed in the case of the mixed biofilm
361 population, with a 2.19 log₁₀ CFU mL⁻¹ reduction in TVC. Analysis of the pre- and post-
362 exposure biofilm populations using VRBA and MSA selective media demonstrated
363 significant inactivation of both bacterial species present in the biofilm, with approximately
364 1.2 and 1.7 log₁₀ CFU mL⁻¹ reductions in *E. coli* and *S. aureus*, respectively, being observed.

365

366 <FIGURE 5>

367

368 <TABLE 2>

369

370 **DISCUSSION**

371

372 Despite the development of new antimicrobial agents and novel sterilisation and disinfection
373 technologies, bacterial biofilms remain a significant problem in both the food industry and
374 clinical settings. The current study has investigated, for the first time, the bactericidal effects

375 of 405-nm light on bacterial biofilms, with results demonstrating successful inactivation of
376 biofilms on both glass and acrylic surfaces, and that the bactericidal effect was observed with
377 both monolayer and mature biofilm populations. Overall, results showed that successful
378 inactivation was achieved with all complexities of *E. coli* biofilms generated on both glass
379 and acrylic, with the general trend demonstrating that the more densely populated the biofilm,
380 the greater the time (and consequently, the greater the dose) required for inactivation.

381

382 As previously discussed, bacterial biofilms can readily form on both glass and plastic
383 surfaces, with production of an extracellular matrix in as little as 4 hours (1,5,30,31,32).
384 Studies have reported stronger initial adhesion between bacteria and hydrophobic surfaces,
385 such as plastics, compared to that of hydrophilic materials, including glass, which may
386 account for initial variations in *E. coli* monolayer biofilm populations. Experimental data
387 from this study highlighted that after 1 hour, *E. coli* attachment to acrylic was greater when
388 compared to that on glass surfaces, however statistical analysis showed this to be
389 insignificant ($P = 0.098$). Slight variation in *E. coli* monolayer biofilm starting populations,
390 after 4 hours development, ($\sim 0.5 \log_{10} \text{CFU mL}^{-1}$) was observed between the glass and
391 acrylic surfaces, which may be an influence of bacterial interactions with surface material
392 properties. Despite this slight difference, investigation into the 405-nm light inactivation of
393 *E. coli* monolayer biofilms on glass and acrylic demonstrated successful results, with near
394 complete bacterial inactivation observed following exposure 20 minutes (approximate dose of
395 168 J cm^{-1}), highlighting the susceptibility of monolayer biofilms to 405 nm light.

396

397 In addition to monolayer biofilms, results demonstrated the successful inactivation of more
398 mature *E. coli* biofilms on both on glass and acrylic surfaces. Population densities of these
399 biofilms ranged from approximately 10^3 – 10^8 CFU mL^{-1} , with the more densely populated

400 biofilms requiring increasing exposure periods for complete inactivation. Biofilms generated
401 on acrylic surfaces over a 24 hour time period required increased exposure time for complete
402 inactivation when compared to those on glass surfaces, despite having significantly lower
403 starting bacterial populations ($\sim 1.5 \log_{10} \text{ CFU mL}^{-1}$ lower). This may be an artefact of the
404 physical adhesive properties between bacteria and specific materials. Chmielewski and
405 Frank (33) reported that although initial bacterial adherence to hydrophobic surfaces is likely
406 to be stronger, greater maximum bacterial adhesion is achieved on hydrophilic surfaces, as a
407 result of high free surface energy, allowing for generation of denser biofilm populations
408 (33,34,35). This information correlates with data shown in this study, with results
409 demonstrating greater adhesion and increased biofilm formation on hydrophilic glass
410 surfaces, following development of mature biofilm structures. Results highlighted that mature
411 biofilms developed over 24 and 48 hour periods had bacterial densities of approximately 4.5-
412 \log_{10} versus 6- \log_{10} CFU mL^{-1} and 5- \log_{10} versus 8- \log_{10} CFU mL^{-1} for hydrophobic and
413 hydrophilic surfaces, respectively.

414

415 Bacterial biofilms generated on both glass and acrylic surfaces over 48 and 72 hours appeared
416 to have similar population densities, suggesting that after the 48-hour growth period, bacterial
417 attachment was maximised and had consequently plateaued. This may be attributed to a lack
418 of nutrients present in the growth media after extended time periods, suggesting media must
419 be replenished to generate increased biofilm populations.

420

421 Successful inactivation of bacterial biofilms on the underside of the glass and acrylic surfaces
422 was also shown, demonstrating the ability of the 405 nm light to transmit through these
423 transparent materials whilst maintaining its antimicrobial activity. With regards to the results
424 of the Weibull analysis, the difference in the inactivation behaviour of “young”, 4-hour

425 monolayer biofilms could potentially be attributed to the different degree of adhesion of
426 microorganism to these acrylic and glass surfaces, with the hydrophobic and hydrophilic
427 interactions between the monolayer biofilms and the surfaces to some extent influencing the
428 inactivation behaviour. However, mature, 24 h, 48 h, and 72 h biofilms don't show similar
429 tendencies. Moreover, their inactivation curves, shown in Figures 2 and 3, demonstrate
430 almost linear behaviour and cannot be fitted with the Weibull's curves (Equation 2).
431 Therefore, it is possible to conclude that with an increase in biofilm 'age' (biofilm thickness
432 and/or number of microorganisms), the influence of substrate material on the inactivation
433 process becomes significantly reduced or disappears completely.

434

435 It is necessary to note that although Equation (2) can be used to fit the experimental
436 inactivation data shown in Figure 4, it is not possible to conclude that the proposed analytical
437 lines are incorrect due to the limited number of experimental data points (only two 405 nm
438 light doses have been used in the present inactivation tests). The present work is aimed only
439 at identification of potential differences in the inactivation behaviour and does not involve a
440 full-scale statistical analysis which requires larger number of experimental data points. It is
441 planned to conduct further direct and indirect tests using a greater number of 405 nm light
442 doses in order to validate the proposed statistical model.

443

444 A variety of methods have been used for biofilm sampling in previous studies including
445 sonication and swabbing (1,36,37,38). Despite all being successful and well utilised methods
446 for recovering microorganisms, each presents its own limitations. Swabbing is a well-
447 recognised method for sampling bacterial contamination within health care and food
448 industrial settings as well as for recovery for bacterial biofilms in laboratory experiments
449 (1,37,38). This method was used throughout this study as a viable and effective technique for

450 bacterial biofilm removal from both glass and acrylic surfaces. Regardless of all inaccuracies/
451 limitations associated with swabbing for bacterial removal, test and control samples in this
452 study were recovered identically using a standard swabbing technique, allowing for directly
453 comparable results.

454

455 The methodology for biofilm formation used in this study was adapted from previous work
456 by Gibson and colleagues (1). The possibility of including a rinsing stage prior to light
457 exposure to ensure all non-attached microorganisms were removed was investigated. Results
458 demonstrated that there was no significant difference between biofilm populations on rinsed
459 and non-rinsed slides, for both monolayer and more mature biofilms ($P>0.08$). Rinsing of test
460 surfaces provided conclusive evidence of biofilm formation as weakly attached cells would
461 have been removed during the rinsing stage. Non-significant reduction in bacterial count
462 following rinsing suggested bacteria were protected, most likely by the presence of an
463 exopolysaccharide matrix which has been shown to protect cells concealed within biofilm
464 layers from harsh environmental conditions such as flowing water (39).

465

466 Previous studies investigating 405-nm light exposure of bacterial suspensions and bacteria
467 seeded onto nutritious surfaces have demonstrated its bactericidal effects (20,40). Studies
468 have indicated that inactivation of Gram-positive bacteria require less exposure time than that
469 of Gram-negative bacteria. Possible explanations for this trend have been accredited to
470 cellular structure, where penetration of light through more structurally complex cells is
471 reduced (41), and variation in the levels of different intracellular porphyrin molecules
472 (40,42). Previous studies have identified numerous porphyrin molecules involved in the
473 photodynamic inactivation of bacteria. A recent study by Dai et al (43) highlighted the
474 presence of both corprotoporphyrin and uroporphyrin in *P. aeruginosa*. Similarly,

475 photoinactivation studies have demonstrated the presence of corpoporphyrin in *S. aureus* and
476 protoporphyrin in *E. coli*, whilst a range of various porphyrin molecules have been associated
477 with *L. monocytogenes* (43,44,45).

478

479 Looking at the results of this study for the inactivation of the four different bacterial species,
480 it can be seen that successful inactivation was achieved with all organisms, with approximate
481 \log_{10} CFU mL⁻¹ reductions of 3.6 and 2.6 for Gram-negative and Gram-positive biofilm
482 populations, respectively. It is, however, difficult in the current study to directly compare the
483 efficacy of 405 nm light for the inactivation of the different bacterial species due to the
484 differences in starting populations observed within the monolayer biofilms. The
485 methodology for preparing the biofilms was kept consistent for the different bacterial species,
486 and this method resulted in the generation of varying populations, possibly reflecting
487 differences in propensity for attachment and/or the rate of multiplication of the attached
488 populations. Variance in bacterial inactivation between the Gram-positive and Gram-negative
489 species (Table 1 and Table 2) may have been a direct effect of the increased adherence of the
490 Gram-positive cells causing increased starting populations, and consequently requiring a
491 greater exposure for complete inactivation, compared to the lower populated Gram-negative
492 biofilms. However, recent data published by Murdoch et al (20) showed that even at similar
493 starting populations, Gram-negative *Salmonella enterica* was inactivated 30% more
494 effectively than Gram-positive *L. monocytogenes* when exposed to 405 nm light whilst
495 seeded onto plastic surfaces (20).

496

497 In addition to investigating single species biofilms, initial tests were carried out to assess the
498 antimicrobial activity of 405 nm light against mixed species biofilms. After a 24h growth
499 period, the population of mixed species biofilm was lower than the populations achieved

500 when compared to the single species biofilms of *E. coli* and *S. aureus*. Analysis of mixed
501 biofilm populations using VRBA and MSA selective media highlighted that although the
502 total population was $\sim 5 \log_{10}$ CFU mL⁻¹, it was found that the ratio between *S. aureus* and *E.*
503 *coli* was uneven, with *S. aureus* being the dominant coloniser (data shown in Table 2). This is
504 likely a direct result of interactions between the bacterial species and competition for
505 attachment. When these mixed biofilms were exposed to 405 nm light, successful inactivation
506 was achieved, with a 2.2 log₁₀ reduction in total population demonstrated. Use of selective
507 media also allowed assessment of the specific populations of *E. coli* and *S. aureus* within the
508 mixed biofilm. VRBA and MSA were chosen for this purpose as they facilitated the selective
509 isolation of *E. coli* and *S. aureus*, respectively, and importantly, these bacteria also act as
510 negative controls when used on the alternative media (46). Results demonstrated that
511 *S. aureus* was the predominant organism to colonise the biofilm, however, successful
512 inactivation of both bacterial species was achieved, with significant reductions achieved in
513 the case of both species. Microscopic examination of the mixed biofilm (Figure 5)
514 highlighted that biofilm distribution was not linear across the entire surface area, but instead
515 displayed many large cellular communities with individual cells dispersed randomly between.
516 Interestingly it was also noted that attachment of *S. aureus* was largely present on top of
517 previously colonised *E. coli* populations, suggesting that *E. coli* may act as a primary
518 coloniser during biofilm formation, highlighting possible roles of cellular interactions during
519 biofilm formation.

520

521 As discussed, the antimicrobial activity of 405 nm light can be attributed to excitation of
522 porphyrin molecules within the cell, leading to production of ROS and oxidative cellular
523 damage (18,22). Recent studies have suggested oxidative damage may directly affect cellular
524 membranes, resulting in reduced membrane stability (47). Interference with the cell

525 membrane and its components may consequently reduce biofilm stability, leading to biofilm
526 degradation through bacterial inability to remain attached to surfaces. It may also be plausible
527 that following 405 nm light exposure, alterations in structural membrane components may
528 possibly prevent cellular attachment and thus prevent biofilm formation. Although this study
529 simply investigated the effects of 405 nm light on the viability of bacterial biofilms once
530 attached to glass and acrylic surfaces, it would be of great interest to investigate the
531 degradative properties of 405 nm light on bacterial biofilms as well as investigating the
532 specific effects of 405 nm light on cellular adhesion. A previous study by Mussi et al. (48)
533 investigated the use of longer blue light wavelengths for inhibition of biofilm formation.
534 Studies have shown many bacteria possess blue light receptors, capable of causing photo-
535 regulated behaviour upon exposure to blue light, and it has been suggested that direct
536 interactions between blue light and subsequent receptors may have inhibitive properties
537 relating to biofilm formation (24,48). However, Mussi and colleagues stated that the effect of
538 light on biofilm formation was inconclusive; highlighting that further work is required to
539 identify any relationship between blue light, blue light receptors and biofilm formation.

540

541 The light irradiance produced by LED array used in this study has a Gaussian distribution, as
542 with many LED-based light systems (49). Highest irradiance is found directly below the
543 centre of the LED array distributing gradually towards the outer edges. Irradiance over the
544 entire test slide was measured (as shown in Figure 1) and the average irradiance was
545 calculated. Although there was a large difference in the measured irradiance at the centre and
546 the outer edges of the slide, the fact that (i) complete inactivation of the biofilm populations
547 could be achieved and (ii) swabs were used to recover bacteria from the entire slide not just
548 the centre point, demonstrated that the inactivation effect was achieved across the entire slide,
549 regardless of the non-uniformity of the light exposure. Although average doses could be

550 calculated, due to the non-uniformity of the irradiance, results (Figures 2, 3 and 4) have been
551 expressed as a function of exposure time. Previous work (25) has shown that 405 nm light
552 microbial inactivation is dose-dependent therefore due to dose being the product of irradiance
553 \times exposure time, the inactivation rates of these biofilms will be increased if an increased
554 irradiance of light is used for exposure.

555

556 The use of light for biofilm decontamination has been extensively investigated, with
557 particular focus on UV-light due to its highly bactericidal properties (8,50). Evidence has
558 suggested that UV-C radiation is largely absorbed by organic materials, such as biofilms,
559 resulting in poor penetration of light and insufficient decontamination (50,51). Short
560 wavelengths in the UV spectrum (200-280nm) present poor penetrability, when compared to
561 that of the visible spectrum. Data shown in Figure 4 highlights the penetrability of 405-nm
562 light, where both direct and indirect exposure of biofilm on glass and acrylic surfaces to 405-
563 nm light produced almost identical inactivation curves. Detrimental properties associated
564 with the use of UV-light are also well recognised, greatly limiting its use for open surface
565 decontamination. With regards to human safety, human exposure to UV radiation is limited
566 due to the associated risk with development of skin and eye cancer (51). Polymer degradation
567 is a further limitation of UV light, imposing financial restraints for continuous repair and
568 replacement of degraded machinery and equipment (52). The safety and operational benefits
569 of 405 nm violet-blue visible light make it suitable for development for both food-related and
570 biomedical decontamination applications for both biofilm and general disinfection purposes.
571 Previous studies have demonstrated the efficacy of 405 nm light for general environmental
572 disinfection (53), but potential uses of violet-blue light also include disinfection of medical
573 devices, and wound decontamination, with a recent study by Dai et al (43) demonstrating the

574 application of blue light for disinfection of *P. aeruginosa* infected burns in mice with no
575 significant damage noted in skin cells.

576

577 In summary, this study has demonstrated for the first time the use of 405-nm light for the
578 inactivation of bacterial biofilms. Biofilms of varying maturity and also of varying bacterial
579 species have been shown to be susceptible to inactivation, demonstrating the ability of the
580 405 nm light to inactivate even densely populated biofilm communities. The ability to
581 inactivate bacterial biofilms present on inert surfaces using 405-nm light is of great
582 significance, and the penetrability of 405-nm light through transparent materials highlights
583 further advantages of this bactericidal light, and demonstrates the potential for development
584 of technologies using 405-nm light for practical decontamination applications within both the
585 food industry and healthcare settings.

586

587 **ACKNOWLEDGEMENTS:** KM wishes to thank The Engineering and Physical Sciences
588 Research Council (EPSRC) for their funding support through a Doctoral Training Grant
589 (awarded in 2010). All authors would like to thank The Robertson Trust for their funding
590 support.

591

592

593

594 **REFERENCES**

595

596 (1) Gibson H., J.H Taylor, K.E Hall, J.T Holah (1999) Effectiveness of cleaning
597 techniques used in the food industry in terms of the removal of bacterial biofilms. *J Appl*
598 *Microbiol*, **87**: 41-48.

599

600 (2) Stewart P.S and J.W Costerton (2001) Antibiotic resistance of bacterial biofilm.
601 *Lancet*, **358**: 135-138.

602

603 (3) Moorthy S and P.I Watnick (2004) Genetic evidence that the *Vibrio Cholerae*
604 monolayer is a distinct stage in biofilm development. *Molecular Microbiology*, **52**: 573-
605 587.

606

607 (4) Stoodley P., S Wilson, L Hall-Stoodley, J.D Boyle, H.M Lappin-Scott, J.W Costerton
608 (2001) Growth and detachment of cell clusters from mature mixed species biofilms. *J*
609 *Appl Environ Micro*, **12**: 5608-5613.

610

611 (5) Donlan M.R. (2002) Biofilms: Microbial Life on Surfaces. *Emerg Infect Dis*, **8**: 881-
612 890.

613

614 (6) Kramer A., I Schwebke and G Kampf (2006) How long do nosocomial pathogens
615 persist on inanimate surfaces? A systematic review. *BMC Infect Dis*, **6**: 130.

616

617 (7) Nathanon, T. (2003) Biofilms and the food industry. *Scientific Commons*, **25**: 807-815.

618

619 (8) Li, Y. (2011) Biofilms and Safety Design Criteria for Food Equipment's. *J Adv Mater*,
620 **203**: 2731-2736.

621

622 (9) Hota S., Z Hirji, K Stockton, C Lemieux, H Dedier, G Wolfaardt, M.A Gardam
623 (2009) Outbreak of multidrug resistant *Pseudomonas aeruginosa* colonization and

624 infection secondary to imperfect intensive care unit room design. *Infect Control Hosp*
625 *Epidemiol*, **30**:25-33.

626

627 (10) Prakash B., B Veeregowda and G Krishnappa (2003) Biofilms: A survival strategy
628 of bacteria. *Curr Sci*, **85**:1299-1307.

629

630 (11) Pflumm M .(2011) Caught on film. *Nature Med*, **17**:650-653.

631

632 (12) Agostinho, AM., A Hartman, C Lipp, A.E Parker, P.S Stewart, G.A James (2011)
633 An in vitro model for the growth and analysis of chronic wound MRSA biofilm. *J Appl*
634 *Microbiol*, **111**: 1275-1282.

635

636 (13) Otto C., S Zahn, F Rost, P Zahn, D Jaros and H Rohm (2011) Physical methods for
637 Cleaning and Disinfection of Surfaces. *Food Eng Rev*, **64**: 367-372.

638

639 (14) Patel R (2005) Biofilms and antimicrobial resistance. *Clin Orthop Rel Res*, NA: 41-
640 47.

641

642 (15) Burmølle MJ., S Webb, D Rao, L.H Hansen, S.J Sørensen, S Kjelleberg (2006)
643 Enhanced biofilm formation and increased resistance to antimicrobial agents and bacterial
644 invasion are caused by synergistic interactions in multispecies biofilm. *J Appl Environ*
645 *Microbiol*, **72**: 3916-3923.

646

- 647 (16) Enwemeka CS., D Williams, S Hollosi, D Yens, S.K Enwemeka (2008) Visible 405
648 nm SLD photo destroys methicillin-resistant *Staphylococcus aureus* (MRSA) in vitro.
649 *Lasers Surg Med*, **40**: 734-737.
- 650
- 651 (17) Maclean M., S.J MacGregor, J.G Anderson and G.A Woolsey (2008) High-intensity
652 narrow-spectrum light inactivation and wavelength sensitivity of *Staphylococcus aureus*.
653 *FEMS Microbiol Lett*, **282**: 227-232.
- 654
- 655 (18) Maclean M., S.J MacGregor, J.G Anderson and G.A Woolsey (2008) The role of
656 oxygen in the visible light inactivation and wavelength sensitivity of *Staphylococcus*
657 *aureus*. *J Photochem Photobiol*, **92**: 180-184.
- 658
- 659 (19) Enwemeka CS., D Williams, S Hollosi, D Yens, S.K Enwemeka (2009) Blue 470nm
660 light kills methicillin-resistant *Staphylococcus aureus* (MRSA) in vitro. *Photomed Laser*
661 *Surg*, **27**: 221-226.
- 662
- 663 (20) Murdoch LE., M Maclean, E Endarko, S.J MacGregor and J.G Anderson (2012)
664 Bactericidal effects of 405 nm light exposure demonstrated by inactivation of
665 *Escherichia*, *Salmonella*, *Shigella*, *Listeria* and *Mycobacterium* Species in liquid
666 suspensions and on exposed surfaces. *Scientific World Journal*, **54**: 1-8.
- 667
- 668 (21) Maclean M, L.E Murdoch, S.J MacGregor, J.G Anderson (2013) Sporicidal effects
669 of 405 nm visible light on endospore forming bacteria. *J Photochem Photobio*. **89**: 120-
670 126.
- 671

- 672 (22) Hamblin M.R and T Hasan (2004) Photodynamic therapy: a new antimicrobial
673 approach to infectious disease? *Photochem Photobiol Sciences*, **5**: 436-450.
674
- 675 (23) Murdoch LE., M Maclean, S.J MacGregor and J.G Anderson (2010) Inactivation of
676 *Campylobacter jejuni* by exposure to high intensity 405 nm visible light. *Foodborne*
677 *Pathog Dis*, **7**: 1211- 1216.
678
- 679 (24) Dai T., A Gupta, C.K Murray, M.S Vrahas, G.P Tegos, M.R Hamblin (2012) Blue
680 light for infectious diseases: Propionibacterium acnes, Helicobacter pylori and beyond?
681 *Drug Resis Update*, **15**: 223-236.
682
- 683 (25) Endarko E., M Maclean, I.V Timoshkin, S.J MacGregor, J.G Anderson (2012) High
684 intensity 405 nm light inactivation of *Listeria monocytogenes*. *J Photochem Photobiol*,
685 **40**: 734-737.
686
- 687 (26) Milton J.S, J.C Arnold (1995) Introduction to probability and statistics, McGraw-
688 Hill, New York.
689
- 690 (27) Van Boekel M. (2002) On the use of the Weibull model to describe thermal
691 inactivation of microbial vegetative cells. *Int J Food Microbiol*, **74**: 139– 159.
692
- 693 (28) Luksiene Z., R Kokstaite, P Katauskis, V Skakaukas (In Press) Novel approach for
694 effective and uniform inactivation of gram-positive *Listeria monocytogenes* and gram-
695 negative *Salmonella enterica* by photosensitization. *Food Techno Biotech*
696

- 697 (29) Schenk M., S Guerrero, S Alzamora, (2008) Response of Some Microorganisms to
698 Ultraviolet Treatment on Fresh-cut Pear, *Food Biopro Technol*, **1**: 384–392.
699
- 700 (30) Habimana O, M Mayrand, T Meylheuc, S Kulakaukas, R Brandet (2009) Genetic
701 features of resistant biofilms determine attachment of *Listeria monocytogenes*. *J Appl*
702 *Environ Microbiol* **75**: 7814-7821
703
- 704 (31) Koseoglu H, G Aslan, N Esen, B.H Sen, H Coban (2006) Ultrastructural stages of
705 biofilm development of *Escherichia coli* on urethral catheters and effects of antibiotics on
706 biofilm formation. *Adu Urol*, **68**: 942-946
707
- 708 (32) Shanks R.M.Q, N.P Donegan, M.L Graber, S.E Buckingham, M.E Zeans, A.L
709 Cheung, G.A O'Toole (2005) Heparin stimulates *Staphylococcus aureus* biofilm
710 formation. *J Infec Immun*, **73**: 4596-4606
711
- 712 (33) Chemleiewski R and J Frank (2003) Biofilm formation and control in food
713 processing facilities. *Comprehensive Reviews in Food Science and Food Safety*, **2**: 22-32.
714
- 715 (34) Hyde F., M Alberg and K Smith (1997) Comparison of fluorinated polymers against
716 stainless steel, glass and propylene in microbial biofilm adherence and removal. *J Ind*
717 *Microbiol Biot*, **19**: 142-149.
718
- 719 (35) Blackman I.C and J Frank (1996) Growth of *Listeria monocytogenes* as a biofilm on
720 various food processing surfaces. *J Food Protect*, **59**: 827-831.
721

- 722 (36) Schaule G., T Griebe, H Fleming (2000) Steps in biofilm sampling and
723 characterisation in biofouling case. *Investigative methods and applications*. ed. Fleming
724 H.C., Szewzyk H.C, Griebe T. pp1-18. Technomic Publishing Company Inc,
725 Pennsylvania.
- 726
- 727 (37) Gibbert Y., M Veillette, C Duchaine (2010) Airborne bacteria and antibiotic
728 resistance genes in hospital rooms. *J Aerobio*, **26**: 185-194.
- 729
- 730 (38) Patted S.M., S Chinagudi, V.R Soragavi, S.B Bhavi (2013) The prevalence of MRSA
731 infection in orthopaedic surgery in a medical college hospital: A 2-year analysis, **1**: 33-
732 35.
- 733
- 734 (39) Scwartz T., W Kohnen, B Jansen, U Obst (2003) Detection of antibiotic resistant
735 bacteria and their resistance genes in waste water, surface water and drinking water
736 biofilms. *FEMS Microbiol Ecol*, **43**: 325-335.
- 737
- 738 (40) Maclean M., S.J MacGregor, J.G Anderson and G.A Woolsey (2009) Inactivation of
739 bacterial pathogens following exposure to light from a 405-nanometre light-emitting
740 diode array. *J Appl Environ Microbiol*, **75**: 1932-1937.
- 741
- 742 (41) Demidova., T.N and M.R Hamblin (2005) Effect of cell-photosensitizer binding and
743 cell density on microbial photoinactivation. *Antimicrob Agents and Chemother*, **49**: 2329-
744 2335.
- 745

746 (42) Guffey J.S., and J Wilborn (2006) In vitro bactericidal effects of 405 nm and 470nm
747 blue light. *Photomed Laser Surg*, **24**: 684-688.

748

749 (43) Dai T., G Asheesh, Y Haung, R Yin, K.C Murray, M.S Vrahas, M Sherwood, G.P
750 Tegos, M.R Hamblin (2012). Blue light rescues mice from potentially fatal *Pseudomonas*
751 *aeruginosa* infection: efficacy, safety and mechanism of action. *Antimicrob Agents*
752 *Chemother*, **57**: 1238-1245

753

754 (44) Nitzan Y and M Kauffman (1999) Endogenous porphyrin production in bacteria by
755 Aminolaevulinic acid and subsequent bacterial photoeradication. *Laser Med Sci*, **14**: 269-
756 277

757

758 (45) Buchovec I., E Paskeviciute, Z Luksiene (2010). Photoinactivation of food pathogen
759 *Listeria monocytogenes*. *Food Tech*, **48**: 207-213

760

761 (46) Bridson E.Y. The Oxoid Manual (1998) 8th Edition. Oxoid Limited, England

762

763 (47) Wasson J.W, J.L Zourelis, N.A Aardsma, J.T Eells, M.T Ganger, J.M Schober, T.A
764 Skwor (2012). Inhibitory effects of 405 nm irradiation on *Chlamydia trachomatis* growth
765 and characterization of the ensuing inflammatory response in HeLa cells. *BMC Microbio*,
766 **12**: 1471-2180

767

768 (48) Mussi M.A., J.A Gaddy, M Cabruja, B.A Arivett, A.M Viale, R Rasia, L.A Actis
769 (2010) The opportunistic human pathogen *Acinetobacter baumannii* senses and responds
770 to light. *J Bacteriol*, **192**: 6336-6345.

771

772 (49) Moreno I., C Sun (2008) Modelling the radiation pattern of LEDs. *Optics Express*,
773 **16**:1808-1819.

774

775 (50) Andersen B.M., H Bånrud, E Bøe, O Bjordal, F Drangsholt (2006) Comparison of
776 UVC light and chemicals for disinfection of surfaces in hospital isolation units. *Infect*
777 *Control Hosp Epidemiol*, **27**: 729-734.

778

779 (51) Matsumura Y and H.N Ananthaswamy (2004) Toxic effects of ultra violet radiation
780 on the skin. *Toxicol Appl Pharmacol*, **195**: 298-308.

781

782 (52) Zhao X., Z Li, Y Chen, L Shi, Y Zhu (2007) Solid phase photocatalytic degradation
783 of polyethene plastic under UV and solar light irradiation. *J Mol Catal*, **268**: 101-106.

784

785 (53) Maclean M., S.J MacGregor, J.A Anderson, G.A Woolsey, J.E Coia, K Hamilton, I
786 Taggart, S.B Watson, B Thakker, G Gettinby (2010) Environmental decontamination of
787 hospital isolation rooms using high intensity narrow spectrum light. *J Hosp Inf*, **76**: 247-
788 251

789

790

791

792

793

794 **Table 1:** Inactivation of bacterial monolayer biofilms on glass surfaces following exposure to
 795 405-nm light.
 796

Bacterial species	Time (min)	Dose (J cm ⁻²)	Non exposed sample (mean log ₁₀ CFU mL ⁻¹)	Exposed sample (mean log ₁₀ CFU mL ⁻¹)	Log reduction (* P≤0.05)	P values
<i>E. coli</i>	0	0	3.55 (±0.02)	3.55 (±0.02)	0	
	5	42	3.52(±0.05)	3.33(±0.05)	0.19	0.07
	10	84	3.39(±0.07)	0.89(±0.58)	2.50*	0.002
	20	168	3.41(±0.11)	0(±0)	3.41*	0.00
<i>P. aeruginosa</i>	0	0	3.58(±0.03)	3.58(±0.03)	0	
	5	42	3.47(±0.01)	1.97(±0.05)	1.5*	0.00
	10	84	3.59(±0.05)	1.16(±0.06)	2.43*	0.00
	20	168	3.72(±0)	0(±0.29)	3.72*	0.00
<i>L. monocytogenes</i>	0	0	4.14(±0.27)	4.14(±0.27)	0	
	5	42	4.10(±0.08)	3.49(±0.57)	0.61*	0.047
	10	84	4.24(±0.16)	3.15(±0.08)	1.09*	0.002
	20	168	4.14(±0.27)	1.66(±0.41)	2.48*	0.001
<i>S. aureus</i>	0	0	5.36(±0.07)	5.30(±0.13)	0	
	5	42	5.32(±0.33)	4.75(±0.06)	0.61*	0.004
	10	84	5.89 (±0.9)	3.45(±0.33)	1.87*	0.00
	20	168	5.36(±0.07)	3.14(±0.09)	2.75*	0.002

797
 798
 799
 800
 801

802 **Table 2:** Inactivation of *E. coli*, *S. aureus*, and mixed *E. coli* and *S. aureus* bacterial biofilms
 803 formed on glass surfaces over a 24 hour period. Counts are provided for total viable counts
 804 (TVC), and in the case of the mixed biofilms, selective counts of *S. aureus* and *E. coli* have
 805 been provide using selective media: (MSA and VRBA).

806

Biofilm	Bacterial	Non-exposed biofilm	Exposed biofilm	Log ₁₀
Species	count	(mean log ₁₀ CFUmL ⁻¹)	(mean log ₁₀ CFUmL ⁻¹)	Reduction
(* P≤0.05)				
<i>E. coli</i>	TVC	5.66	1.29	4.37*
<i>S. aureus</i>	TVC	6.31	3.34	2.97*
Mixed	TVC	5.29	3.09	2.19*
	MSA	4.30	2.63	1.67*
	VRBA	2.29	1.10	1.19*

807

808

809

810

811

812

813

814

815

816

817

818

819 **FIGURE CAPTIONS**

820

821 **Figure 1:** Three dimensional model simulating the irradiance distribution of the 405 nm light
822 across the glass and acrylic test surfaces (60×25 mm), plotted using OriginPro 8.1 software.

823

824 **Figure 2:** Inactivation of *E. coli* biofilms on glass surfaces following exposure to 405 nm
825 light with an irradiance of ~ 140 mW cm², given as a function of time. Biofilms were allowed
826 to develop for 4, 24, 48 and 72 hours before light exposure. * Indicates statistically
827 significant differences when compared to control samples ($P \leq 0.05$).

828

829 **Figure 3:** Inactivation of *E. coli* biofilms on acrylic surfaces following exposure to 405 nm
830 light with an irradiance of ~ 140 mW cm², given as a function of time. Biofilms were allowed
831 to develop for 4, 24 and 48 hours before light exposure. * Indicates statistically significant
832 differences when compared to control samples ($P \leq 0.05$).

833

834 **Figure 4:** Inactivation of *E. coli* monolayer biofilms on (a) glass and (b) acrylic, by direct
835 (\blacktriangle) and indirect (\square) exposure to 405 nm light. Indirect exposure investigated transmission
836 of the 405 nm light through the slides to inactivate biofilms on the underside of the slides.
837 The average irradiance of 405 nm light across the slides was approximately 140 mW cm⁻²,
838 reducing by $\sim 4\%$ when transmitted through the slide. Results are given as a function of time.
839 * Indicates a statistically significant difference when compared to control samples ($P \leq 0.05$).
840 No significant difference was observed between direct and indirect inactivation on both
841 surfaces. Weibull analytical fit lines are shown as inset graphs and were obtained using
842 Equation (2).

843

844 **Figure 5:** Microscopic visualisation of a Gram stain of a mixed species biofilm consisting of
845 *S. aureus* and *E. coli* after 24 hour development. Cells were viewed under oil immersion at
846 ×1000 magnification.

847

848

849

850

851

852

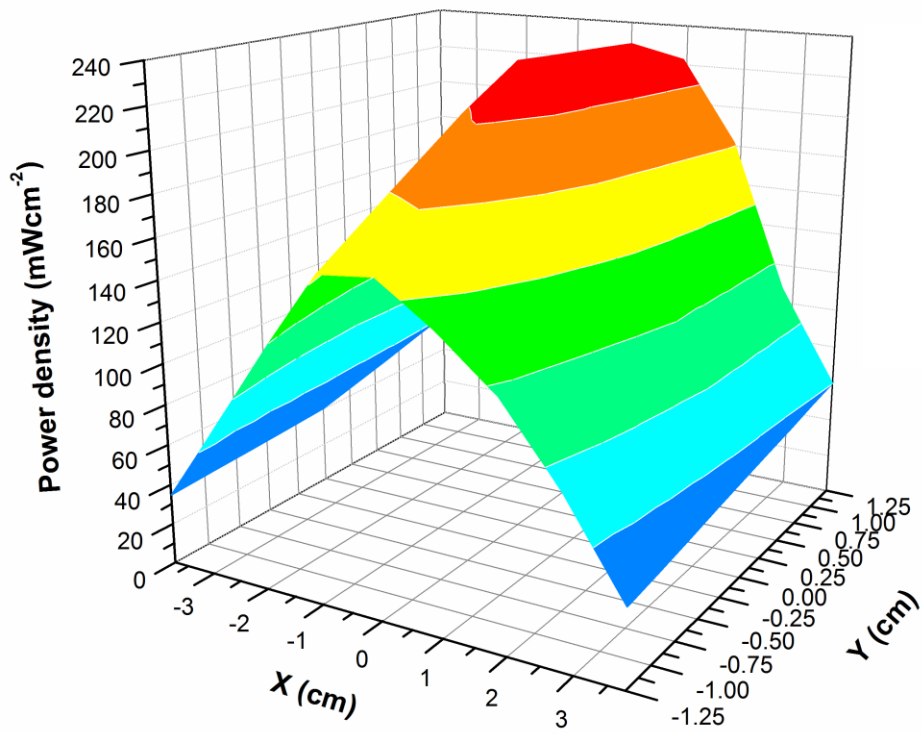
853

854

855

856

857



858

859 Figure 1

860

861

862

863

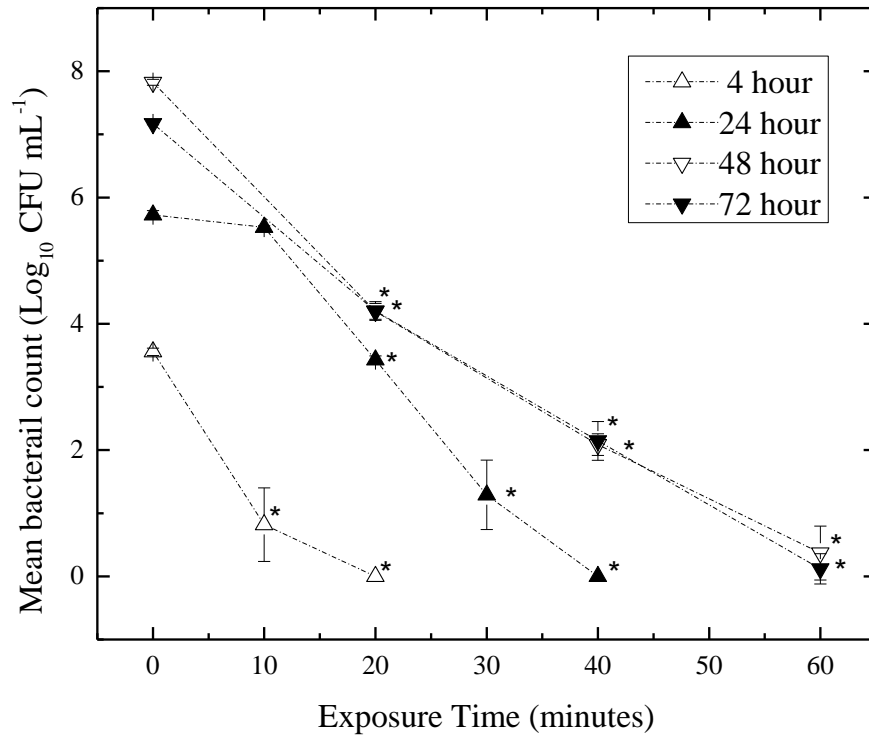
864

865

866

867

868



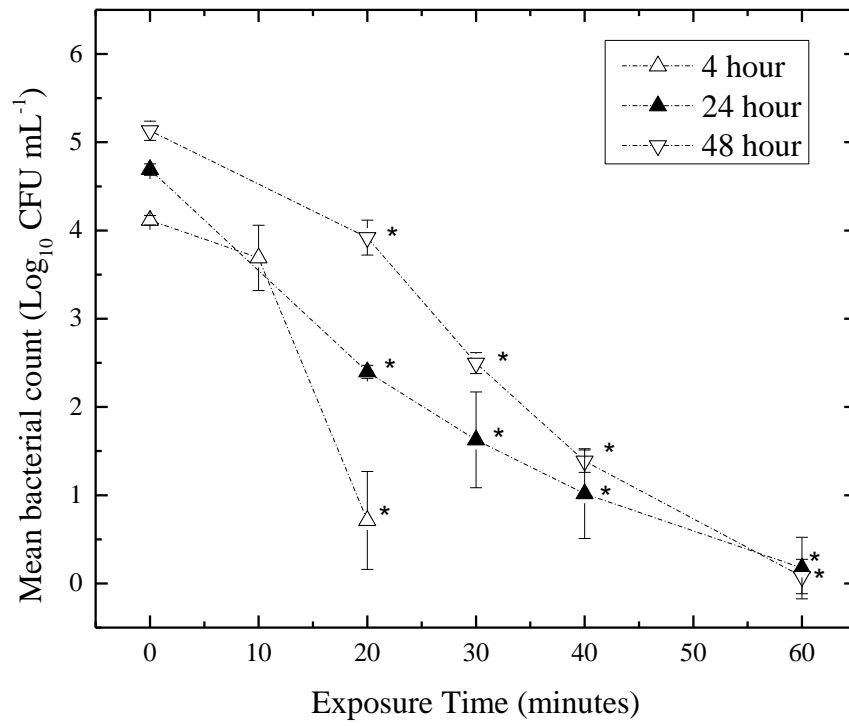
869

870

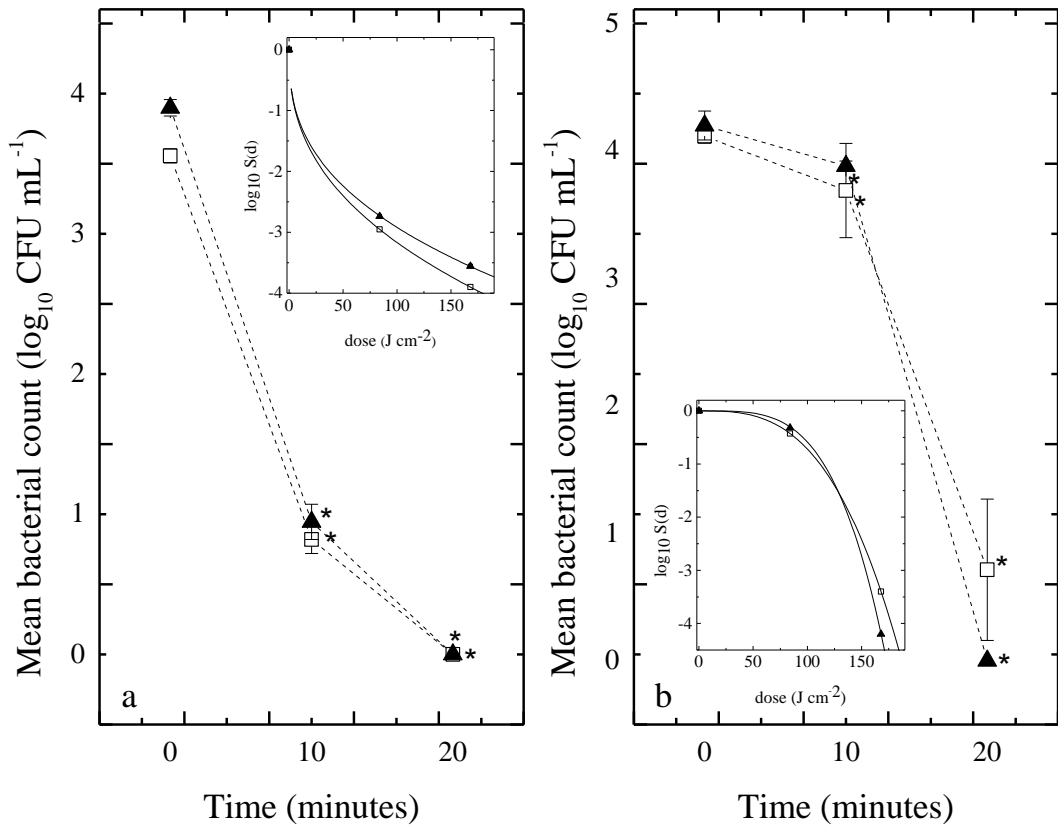
871

872

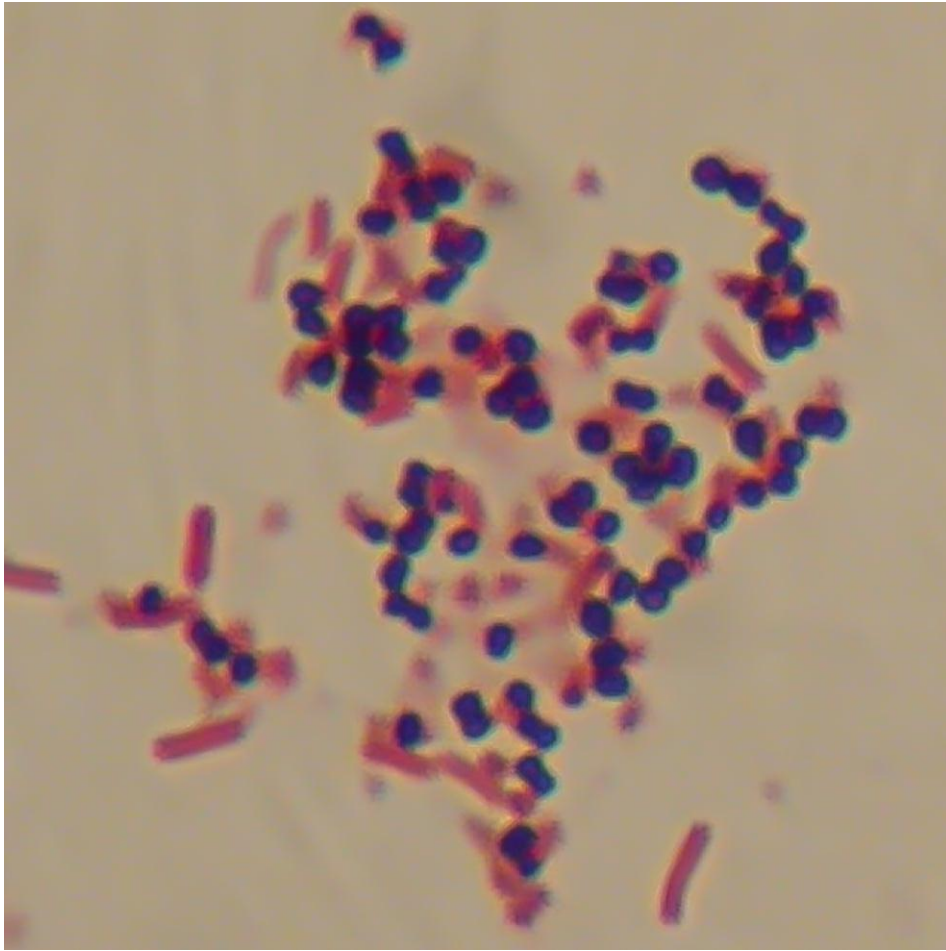
Figure 2



873
 874 Figure 3
 875



876
877 Figure 4
878



879
880
881

Figure 5